

# Precision of Hubble constant derived using black hole binary absolute distances and statistical redshift information

Chelsea L. MacLeod and Craig J. Hogan  
*University of Washington,  
 Department of Astronomy, Box 351580  
 Seattle, WA 98195-1580*  
 (Dated: February 2, 2008)

Measured gravitational waveforms from black hole binary inspiral events directly determine absolute luminosity distances. To use these data for cosmology, it is necessary to independently obtain redshifts for the events, which may be difficult for those without electromagnetic counterparts. Here it is demonstrated that certainly in principle, and possibly in practice, clustering of galaxies allows extraction of the redshift information from a sample statistically for the purpose of estimating mean cosmological parameters, without identification of host galaxies for individual events. We extract mock galaxy samples from the 6th Data Release of the Sloan Digital Sky Survey resembling those that would be associated with inspiral events of stellar mass black holes falling into massive black holes at redshift  $z \approx 0.1$  to  $0.5$ . A simple statistical procedure is described to estimate a likelihood function for the Hubble constant  $H_0$ : each galaxy in a LISA error volume contributes linearly to the log likelihood for the source redshift, and the log likelihood for each source contributes linearly to that of  $H_0$ . This procedure is shown to provide an accurate and unbiased estimator of  $H_0$ . It is estimated that a precision better than one percent in  $H_0$  may be possible if the rate of such events is sufficiently high, on the order of 20 to  $z = 0.5$ .

PACS numbers: 98.80.Es

## I. PRECISION COSMOLOGY FROM BLACK HOLE BINARIES

A low frequency gravitational wave detector, such as LISA, is capable of measuring very high signal to noise waveforms from inspirals and mergers of cosmologically distant black hole binaries. From the measured waveform alone it is possible to estimate the parameters of a binary with high precision, including its direction on the sky and its absolute luminosity distance [1]. Aside from numerical factors, the absolute radius of the final hole is fixed by the square of the orbital period divided by the orbit decay or chirp time; the distance is this absolute length divided by the measured wave amplitude. The gravitational calibration of distance is not accompanied by the usual systematics associated with astronomical modeling; indeed it does not even require Standard Model physics. Since a single black hole binary merger can provide distances with absolute precision much better than one percent, this capability may offer a potentially transformative tool for precision measurement of cosmological parameters [2, 3] (for reviews on gravitational waves see Ref.s [4, 5, 6, 7]). Precision measurement of an absolute distance scale, as embodied in the Hubble constant, is important for breaking degeneracies in estimates of cosmological parameters (such as those characterizing cosmological curvature and Dark Energy) using other datasets, such as cosmic background radiation anisotropy [8, 9].

On the other hand there are obstacles in practice to applying the technique. One problem is distance errors added by gravitational lensing along the line of sight [10]. The best raw distances are given by massive black

hole (MBH) binary inspiral events (where both holes are larger than  $10^4 M_\odot$  say), many of which will be measured with very high signal-to-noise ratio [3, 11, 12, 13, 14, 15]. They are predicted to be fairly frequent (one or two events per week on average) and should be observable with LISA out to redshifts greater than 10 [16, 17]. Unfortunately most of the observable events are predicted to occur at redshifts greater than 2 where errors due to lensing are substantial. Thus one is led to consider another class of events, stellar mass black holes inspiralling into massive black holes (the so-called extreme mass ratio inspiral or EMRI events [18, 19, 20, 21, 22]), which occur frequently in galaxies at  $z < 1$  where lensing errors are subdominant. Although the intrinsic precision of these distances is lower due to lower signal-to-noise ratio, they still may provide a unique and precise cosmological probe.

The other major uncertainty is associated with measuring the redshifts of the events. The gravitational waveform provides a measurement of luminosity distance, and a cosmological probe such as a mean redshift-distance relation requires an independent measurement of redshift. In the case of MBH events, it may be possible to identify the host galaxy by seeking electromagnetic counterparts [23, 24, 25, 26, 27, 28, 29] to the merger, such as optical or x-ray variability in accretion disks from the rapid evolution in the gravitational potential of the binary black hole, or even from the sudden removal of several percent of  $Mc^2$  in gravitational radiation at the moment of merger. But in the case of EMRI events, no compelling model requiring an electromagnetic counterpart has been offered: it may be possible to merge a small black hole with a large one with practically no signature aside from the gravitational radiation itself.

The point of this paper is to sketch and demonstrate a technique for measuring cosmological parameters such as the Hubble constant  $H_0$  by obtaining only statistical information about the redshifts of the EMRI hosts, even without identifying the host galaxy of any individual event. For each event, the estimate of direction  $\vec{\theta}$  and distance  $D_L$ , together with a cosmological model relating  $D_L$  and redshift  $z$  roughly estimated from other techniques, provide a three-dimensional “error box” in  $\vec{\theta}, z$  space. As first noted in [1], a galaxy redshift survey in this error box then provides a statistical estimate of the host redshift, since galaxies are highly clustered with each other. Here we demonstrate using a real survey a technique for estimating the likelihood distribution of the host galaxy redshift, which is more accurate (statistically) than the prior information on  $H_0$  that went into constructing the error box.

In order to demonstrate the utility of this technique in practice, we construct mock LISA error boxes in the Sloan Digital Sky Survey (SDSS) volume [30, 31, 32, 33, 34, 35, 36] and generate mock redshift surveys from samples of SDSS galaxies that have about the same statistical clustering properties as a host galaxy population of LISA EMRI sources. One reason to choose a real galaxy survey rather than a simulation for these realizations is that the higher order correlations between galaxies in the cosmic web, which are important for determining the likelihood distribution of redshifts, are known to be correct, as long as the SDSS catalog selection approximates an unbiased sample of a typical EMRI host galaxy population. We find that with enough events, precision better than one percent is possible in measuring the mean redshift-distance relation. This translates into comparable precision in  $H_0$ , by a technique that shares very few systematic errors or biases with other means of measuring  $H_0$ . It also enables other new cosmological tests, for example, direct measurement of cosmic acceleration within the redshift range ( $z < 0.5$ ) where the universe is dominated by Dark Energy.

## II. USE OF STATISTICAL REDSHIFTS FOR COSMOLOGICAL PARAMETER ESTIMATION FROM GRAVITATIONAL WAVEFORMS

A fit to a gravitational wave signal from a black hole inspiral event  $j$  leads to a likelihood distribution  $\ln \mathcal{L}_j(\vec{\theta}, D_L)$  for its angular location  $\vec{\theta}$  and luminosity distance  $D_L$ . We wish to combine this with information from the directions and redshifts of galaxies to measure mean cosmological parameters such as the Hubble constant  $H_0$ .

For the simple realizations shown in Section III., the selection function is highly idealized: all galaxies are assumed to be equally likely hosts, within a certain error box: the angular size of the box is defined by LISA errors in angle, and the depth of the box is determined primarily by prior errors on  $H_0$  from other sources. For

this discussion, intended only to estimate typical errors, we also assume linear Hubble flow, in particular negligible cosmic acceleration (though this is taken into account where needed in the scaling exercise below; the linear discussion is valid as long as acceleration is negligible within each redshift error box). With this simple selection and expansion model, the log-likelihood distribution for the Hubble constant for each event  $j$  is (up to a constant numerical factor)

$$\ln \mathcal{L}_j(H_0) = N_j^{-1} \sum_i \ln \mathcal{L}_j(D_j = cz_i/H_0), \quad (1)$$

summed over the galaxies  $i$  in the box, and for a whole sample,

$$\ln \mathcal{L}(H_0) = \sum_i \sum_j N_j^{-1} \ln \mathcal{L}_j(D_j = cz_i/H_0), \quad (2)$$

where a normalization factor  $N_j$ , the number of galaxies actually measured in each box, is included so that each event is weighted equally independent of the number of galaxies measured. Thus each galaxy gets to vote appropriately on its source redshift, while each EMRI source contributes on an equal footing to estimating a value for  $H_0$ .

If the redshift distribution were very smooth on the scale of the LISA error boxes, this technique would not return useful information on redshift: the likelihood distribution of  $H_0$  would be the same as that going into construction of the error boxes. However, actual galaxies are highly clustered so if the angular errors are not too large, there is recoverable statistical information on  $z$  as demonstrated quantitatively below.

There is a possibility of some bias in the estimate of  $H_0$ , for example if the rate of EMRIs is rapidly evolving with redshift, which means the weighting within each box should not be uniform in  $z$ . Since the mean evolution will actually be measured, such biases can be measured and accounted for statistically; however, we do not model them here.

## III. MOCK LISA/EMRI HOST-GALAXY SAMPLES FROM SDSS

If galaxies are sufficiently clustered, then within the region of  $\vec{\theta}_i, D_i$  allowed for each event, a redshift catalog can give an estimate of the host redshift without knowing which galaxy is the host. The question is whether for realistic galaxy clustering and LISA error boxes, there is enough redshift information to be useful. We answer this question by generating mock redshift samples from regions of the SDSS volume scaled assuming standard cosmology to have about the same clustering properties as EMRI hosts.

We use estimates of LISA errors in distance and sky position from Cutler (private communication). For

$10 + 10^6 M_\odot$  EMRIs at a redshift  $z$ , and a fully functioning LISA with two effective synthetic interferometers, we use an error box with a solid angle  $\Delta\theta^2 \approx 4z^2$  square degrees, and assume distance error  $\Delta \ln(D_L) \approx 0.05z$ . For a LISA with only one synthetic interferometer, we adopt  $\Delta\theta^2 \approx 16z^2$  square degrees, and  $\Delta \ln(D_L) \approx 0.07z$ . It should be noted that these estimates only define a 63% confidence interval; therefore, in a proper simulation one should increase the size of the error box by some amount to improve the confidence limits. However, in our exploratory analysis we neglect this correction.

To generate a mock EMRI catalog, a galaxy is selected at random in the SDSS catalog and an error box is generated centered at this redshift and direction. Examples of simulated error boxes for the single synthetic interferometer case are shown in Fig. 1. While the ranges in right ascension and declination are calculated using Cutler’s estimates above, the range in redshift corresponds to an error in  $H_0$  of about 7% (representing a cosmological prior obtained from other techniques). A histogram is then generated from the SDSS galaxies in this box, with the originally selected host galaxy removed. (Thus we assume that the actual host may not even be a visible galaxy, only that it correlates with other galaxies in the usual way.) This gives the likelihood distribution for the EMRI host redshift and, according to (1), gives  $\ln \mathcal{L}_j(H_0)$  for this event. Assuming a value  $H_0 = 70 \text{ km s}^{-1} \text{ Mpc}^{-1}$ , a linear Hubble’s Law, and the same distance for all galaxies in the box (calculated from the host redshift), we convert redshifts into Hubble units. Thus our histograms display a likelihood distribution for  $H_0$  estimated for a sample, which should be compared with a “true” value of  $70 \text{ km s}^{-1} \text{ Mpc}^{-1}$ .

To simulate the LISA distance error for each source, each individual histogram is displaced by a random amount, selected from an interval corresponding to an error of  $\Delta H_0/H_0 = 0.05z$  for two synthetic interferometers, and  $\Delta H_0/H_0 = 0.07z$  for one synthetic interferometer. As an example for the one interferometer case, given a redshift of 0.2 the error would be  $\Delta H_0 = 0.98 \text{ km s}^{-1} \text{ Mpc}^{-1}$ , and the histogram (that is, each “box”) is displaced by a random amount between  $-0.49$  and  $+0.49$  in  $H_0$ . This error is applied before establishing the edges of the histogram at  $H_0 = 65$  and  $H_0 = 75 \text{ km s}^{-1} \text{ Mpc}^{-1}$ , so that new galaxies are allowed to enter the histogram due to the shift in  $H_0$ .

A set of such samples can be combined by stacking their histograms (appropriately normalized to give all events equal weight independent of the number of galaxies in their sample, as in (1)). Since each box is generated with the originally chosen source galaxy assuming  $H_0 = 70 \text{ km s}^{-1} \text{ Mpc}^{-1}$ , a peak should emerge around this value in the stacked histogram. The width of the summed distribution measures the width of the distribution of galaxies, and the offset of the fitted mean from the center ( $70 \text{ km s}^{-1} \text{ Mpc}^{-1}$ ) measures the actual offset in the “measured” from the “true” value of  $H_0$  for each set of realizations.

Results of several mock realizations are displayed in Fig. 2. For each of these sums, 20 “EMRIs” were randomly selected in the SDSS (DR6) spectroscopic survey volume (673,264 galaxies total, classified spectroscopically), excluding the distant part of the survey where galaxy selection is dominated by different criteria. The (spectroscopic) redshifts were limited to  $0.02 \leq z \leq 0.23$ , and all mock error boxes were limited to the regions of the northern galactic cap covered by DR6 (shown on the SDSS website, which is listed under ‘Acknowledgements’). The SDSS provides a statistically complete sample for galaxies with r-band Petrosian magnitudes  $r \leq 17.77$  [32]. In our analysis we neglect peculiar velocities of galaxies, which are likely to add errors of less than about 1% per object even for the nearest plausible samples and are therefore subdominant.

Each individual error box that was constructed yields  $\ln \mathcal{L}_j(H_0)$ , displayed as a histogram which plots the number of galaxies versus  $H_0$ . The originally chosen source galaxy was subtracted from each histogram, and therefore error boxes that contained only the chosen source galaxy were ignored. This is reflected in the final box count (the initial box count is 20), which is listed above each plot. Each of these histograms were then normalized by dividing by the total number of galaxies contained in each error box ( $N_j$ ), not including the original source galaxy. Individual histograms were then added together, resulting in a plot of  $\ln \mathcal{L}(H_0)$  that contains information purely from galaxy clustering.

The results from these realizations are summarized in Table I, where the average redshift of the chosen source galaxies is included, as well as the total number of galaxies used in the summed histogram. It can be seen that the samples cluster near the “true” value of  $70 \text{ km s}^{-1} \text{ Mpc}^{-1}$  and would allow a measurement of  $H_0$  with a typical error in the mean of about  $0.2 \text{ km s}^{-1} \text{ Mpc}^{-1}$  (averaged over 25 realizations for the one interferometer case), or a precision of about one third of a percent. This shows that the statistical redshift technique is credible with a realistic galaxy distribution and LISA errors.

As expected, the distribution of candidate Hubble constants is highly nongaussian, so a sample at least this large is needed for a reliable result. In order to get a sample of order 10 or more EMRIs at such a low redshift, the overall rate of EMRIs would have to be at the high end of current estimates [22].

Therefore, in a second round of experiments, we tested the reliability of the above technique for larger redshifts, still using the same SDSS data (with  $z$  limited to  $0.02 \leq z \leq 0.23$ ) but scaling to estimate higher redshift behavior in the same galaxy population. We chose to scale to higher  $z$  from this SDSS range since the SDSS does not sample typical galaxy populations at  $z \gtrsim 0.23$ .

Adopting a larger redshift value for a fiducial EMRI event increases the LISA angular and distance errors according to Cutler’s estimates, and at the same time requires a scaling of the SDSS data in order to estimate the properties of a similarly-clustered galaxy host

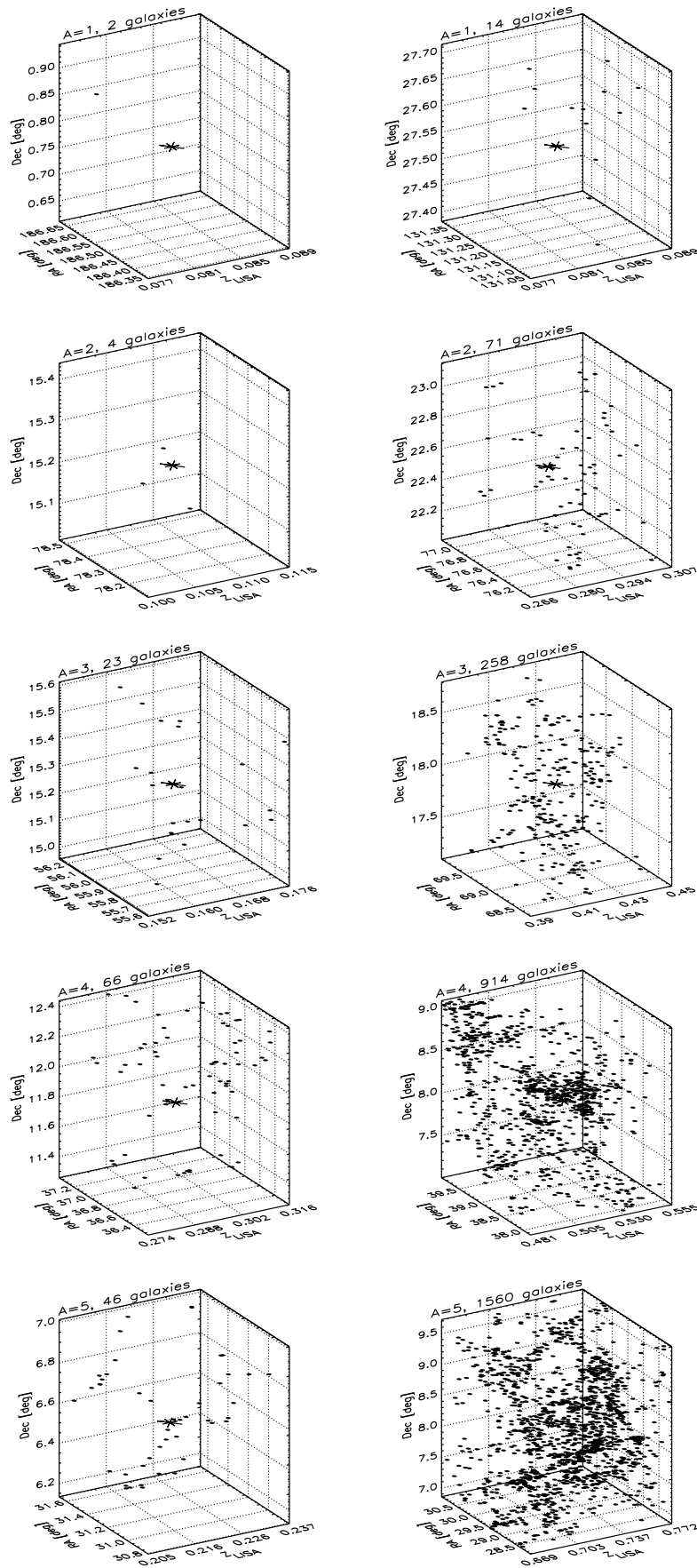


FIG. 1: Simulated LISA error boxes for one synthetic interferometer. In each box the chosen source galaxy lies at the center, indicated by an asterisk, and dots represent all other galaxies in the box. Boxes are scaled to represent events at  $z_{LISA} = Az_{SDSS}$ , where  $A$  is specified above each box, and the pretend LISA angular coordinates, given by  $\theta_{LISA} = (1/A)\theta_{SDSS}$ , are plotted.

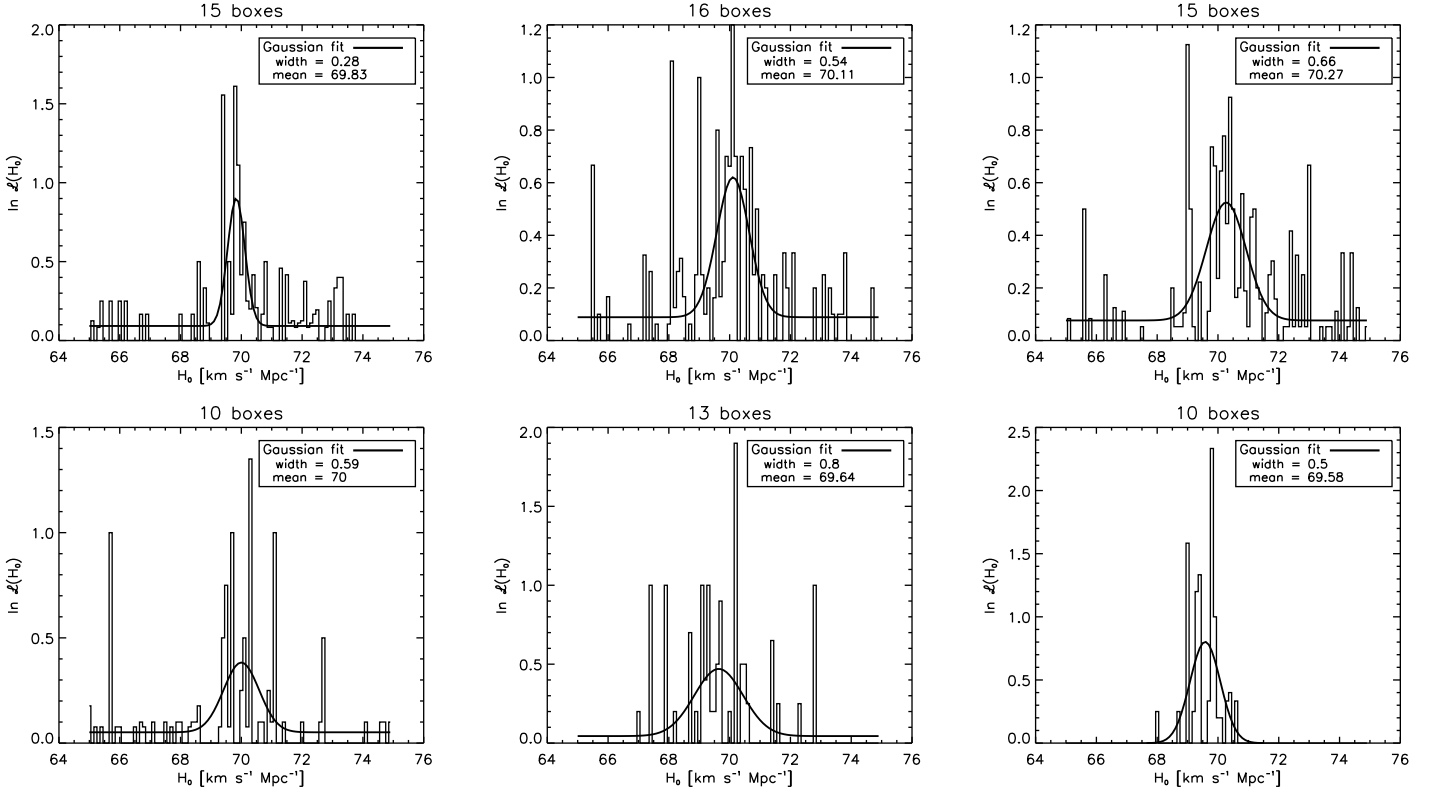


FIG. 2: Summed histograms (bin size = 0.1) with Gaussian fits overlaid. Top row: one synthetic interferometer case; bottom row: two synthetic interferometers. The true value of  $H_0$  was assumed to be  $70 \text{ km s}^{-1} \text{Mpc}^{-1}$ . Gaussian fits were generated using a Levenberg-Marquardt technique to iteratively search for a best least-squares fit to  $\ln \mathcal{L}(H_0)$ . The starting value for the mean was a random value between 68 and 72, and those for the width and area were both 1. Vertical axes are in arbitrary units.

TABLE I: Results for realizations in Fig. 2; starting from top left.

Number of Boxes (Sources)	Average $z$	$\Sigma N_j$	Width of Gaussian	Mean $H_0$ [ $\text{km s}^{-1} \text{Mpc}^{-1}$ ]
15	0.125	72	0.28	69.83
16	0.109	74	0.54	70.11
15	0.135	103	0.66	70.27
10	0.119	46	0.59	70.00
13	0.113	32	0.80	69.64
10	0.114	21	0.50	69.58

population at larger redshift. For one synthetic interferometer, Cutler's estimates give us an angular error  $\Delta\theta_{LISA} = 4z_{LISA}$  degrees on each side of an error box. When scaling by a factor  $A$  to a source redshift  $z_{LISA} = Az_{SDSS}$ , where  $z_{SDSS}$  is the redshift of a random host galaxy in SDSS, the LISA angular error is

$$\Delta\theta_{LISA} = 4Az_{SDSS} \text{ degrees.} \quad (3)$$

To estimate the angle corresponding to the galaxy structure at higher redshift in this angular box, we assume a  $\Lambda$ CDM cosmology with a few simplifications. Assume that the galaxy distribution is frozen in comoving coor-

dinates, which is approximately true in a  $\Lambda$  dominated universe. Then a structure that has an angular size  $\theta_{LISA}$  at redshift  $z_{LISA}$  will appear at  $z_{SDSS}$  with an angular size

$$\theta_{SDSS} = \theta_{LISA}(D_{LISA}/D_{SDSS})[(1+z_{LISA})/(1+z_{SDSS})] \quad (4)$$

where angular size distances are denoted by  $D$ . One can verify numerically in  $\Lambda$ CDM that within 10%, this agrees with a simple formula,

$$\theta_{SDSS} = \theta_{LISA}(z_{LISA}/z_{SDSS}), \quad (5)$$

which can be obtained by using a small  $z$  expansion and

neglecting higher order terms in  $z$  (which is appropriate since the range in  $z$  in a LISA error box is small). Therefore, combining (3) and (5), the angular size we use on one side of an SDSS error box in our scaled realizations scales as

$$\Delta\theta_{SDSS} = \Delta\theta_{LISA}A = 4A^2z_{SDSS} \text{ degrees.} \quad (6)$$

The LISA distance error was taken into account using the same method as before, except now scaled to  $\Delta \ln(D_L) \approx 0.07Az_{SDSS}$  for one synthetic interferometer. The results of these realizations are shown in Fig. 3, where scalings of  $A=2, 3, 4$ , and  $5$  were used.

Results are summarized in Table II. It can be seen that these are much more realistic than the lower-redshift realizations, with typical boxes containing hundreds of EMRI host tracer galaxies. Nevertheless, the final  $H_0$  estimate remains precise even for redshifts out to  $z_{LISA} = 0.5$ . It should be noted that since these error boxes are much larger and are still limited to the northern galactic cap, significant overlapping of error boxes occurs when scaling to high redshift, primarily for  $A = 5$ . Therefore, the results for these cases are not as reliable due to lack of independence.

It should also be noted that even for these larger error boxes, there are still cases where few galaxies ( $< 10$ ) are contained within a box, and occasionally there will only be one to two galaxies. These galaxies contribute significantly to the final, summed histograms. Figure 4 shows histograms of the number of galaxies contained in each box, that is, the distributions of  $N_j$  values, for each of the plots in Fig. 3.

The resulting errors in the mean ( $\delta_{H_0} = |70 - \text{mean}|$ ) averaged over 25 realizations for each value of  $A$  are listed in Table III, all for the single synthetic interferometer case.

In conclusion, we have found that if LISA detects 20 or more EMRI events to a redshift of  $z \approx 0.5$ , galaxy

surveys of the LISA error boxes are likely to yield a reliable estimate of the Hubble constant to better than one percent precision. A higher rate of EMRI events would permit estimates of cosmic acceleration from the redshift-distance relation in this redshift range with considerably more precision than other known techniques.

### Acknowledgements

Funding for the Sloan Digital Sky Survey (SDSS) and SDSS-II has been provided by the Alfred P. Sloan Foundation, the Participating Institutions, the National Science Foundation, the U.S. Department of Energy, the National Aeronautics and Space Administration, the Japanese Monbukagakusho, and the Max Planck Society, and the Higher Education Funding Council for England. The SDSS Web site is <http://www.sdss.org/>.

The SDSS is managed by the Astrophysical Research Consortium (ARC) for the Participating Institutions. The Participating Institutions are the American Museum of Natural History, Astrophysical Institute Potsdam, University of Basel, University of Cambridge, Case Western Reserve University, The University of Chicago, Drexel University, Fermilab, the Institute for Advanced Study, the Japan Participation Group, The Johns Hopkins University, the Joint Institute for Nuclear Astrophysics, the Kavli Institute for Particle Astrophysics and Cosmology, the Korean Scientist Group, the Chinese Academy of Sciences (LAMOST), Los Alamos National Laboratory, the Max-Planck-Institute for Astronomy (MPIA), the Max-Planck-Institute for Astrophysics (MPA), New Mexico State University, Ohio State University, University of Pittsburgh, University of Portsmouth, Princeton University, the United States Naval Observatory, and the University of Washington.

- 
- [1] B. F. Schutz, *Nature (London)* **323**, 310 (1986).
  - [2] N. Dalal, D. E. Holz, S. A. Hughes, and B. Jain, *Phys. Rev. D* **74**, 063006 (2006).
  - [3] D. E. Holz and S. A. Hughes, *Astrophys. J.* **629**, 15 (2005).
  - [4] E. Flanagan and S. Hughes, *New J. Phys.* **7**, 204 (2005).
  - [5] C. J. Hogan, in *Frontiers of Astrophysics: A Celebration of NRAO's 50th Anniversary*, Charlottesville, 2007, edited by A. H. Bridle, J. J. Condon and G. C. Hunt (to be published); Report No. arXiv:0709.0608v2, 2007.
  - [6] P. Amaro-Seoane, J. R. Gair, M. Freitag, M. C. Miller, I. Mandel, C. J. Cutler, and S. Babak, *Class. and Quantum Grav.* **24**, 113 (2007).
  - [7] See *Laser Interferometer Space Antenna: 6th International LISA Symposium*, edited by S. M. Merkowitz and J. C. Livas (Greenbelt, 2006) [AIP Conf. Proc. **873**].
  - [8] W. Hu, in *ASP Conf. Ser.* **399**, edited by S. C. Wolff and T. R. Lauer (San Francisco, 2005), p. 215.
  - [9] L. Knox, *Phys. Rev. D* **73**, 023503 (2006).
  - [10] S. A. Hughes and D. E. Holz, *Class. and Quantum Grav.* **20**, 65 (2003).
  - [11] M. Trias and A. M. Sintes, *Phys. Rev. D.* (submitted); Report No. arXiv:0707.4434, 2007.
  - [12] E. Berti, A. Buonanno, and C. M. Will, *Phys. Rev. D* **71**, 084025 (2005).

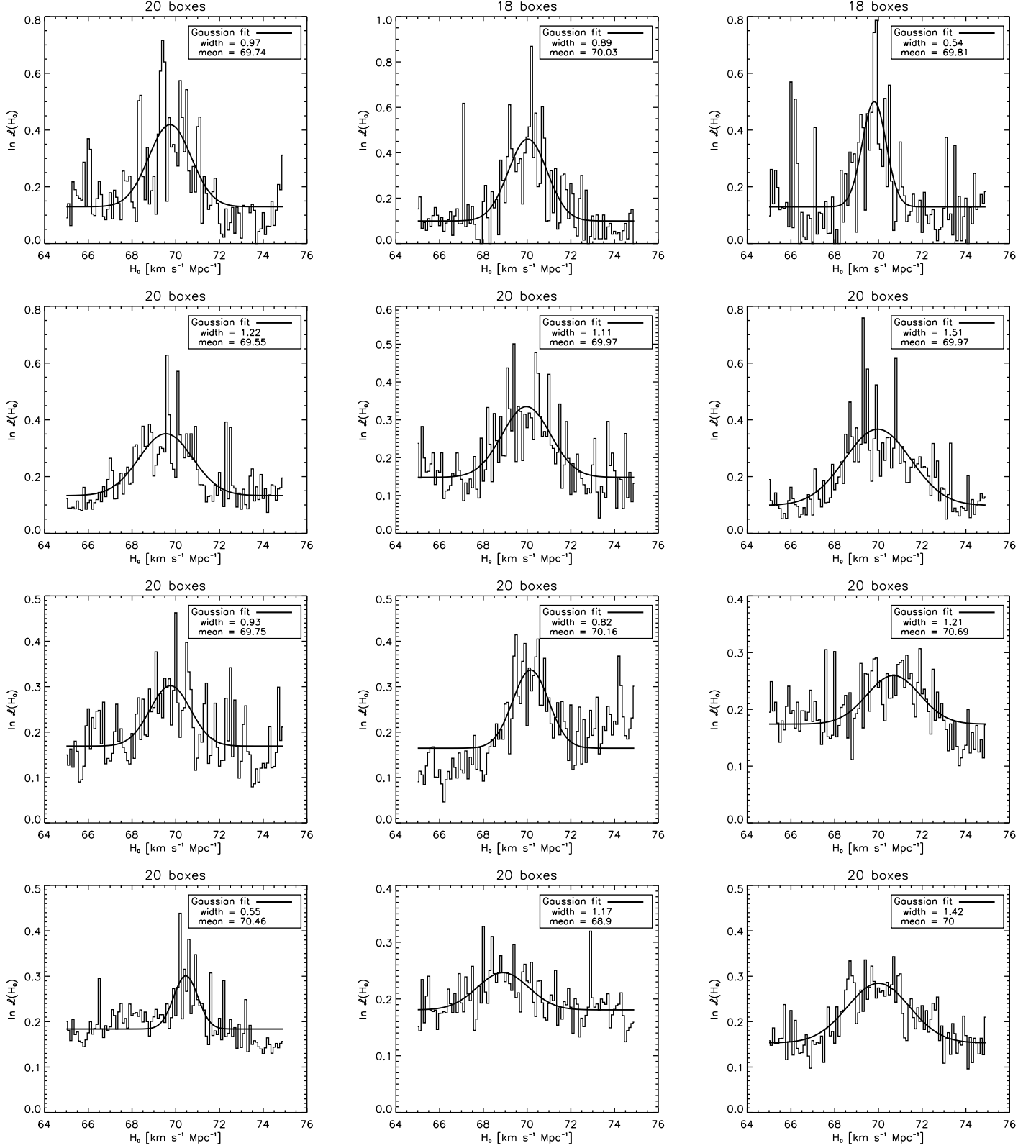


FIG. 3: Summed histograms for one synthetic interferometer, scaled to represent events at  $z_{LISA} = 2z_{SDSS}$  (top row),  $z_{LISA} = 3z_{SDSS}$  (second row),  $z_{LISA} = 4z_{SDSS}$  (third row), and  $z_{LISA} = 5z_{SDSS}$  (bottom row). Vertical axes are in arbitrary units.

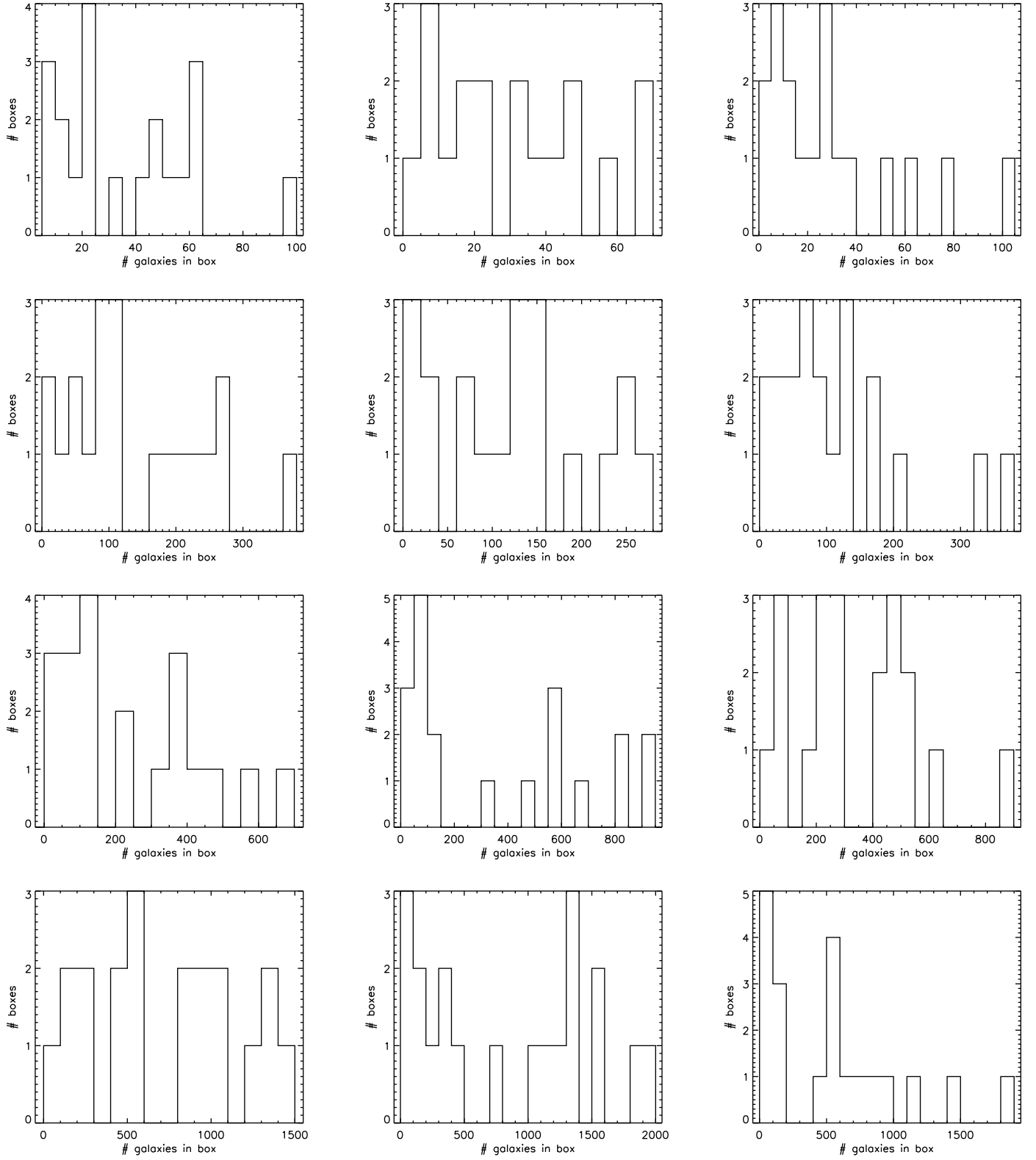


FIG. 4: Distributions of  $N_j$  values for realizations in Figure 3 (in the same order).



TABLE II: Results for realizations in Fig. 3; starting from top left and going through each row left to right.

$A$	Number of Boxes (Sources)	Average $z_{SDSS}$	Average $z_{LISA}$	$\Sigma N_j$	Width of Gaussian	Mean $H_0$ [km s <sup>-1</sup> Mpc <sup>-1</sup> ]
2	20	0.115	0.231	712	0.97	69.74
2	18	0.103	0.206	532	0.89	70.03
2	18	0.105	0.211	525	0.54	69.81
3	20	0.111	0.333	2783	1.22	69.55
3	20	0.115	0.344	2454	1.11	69.97
3	20	0.088	0.263	2320	1.51	69.97
4	20	0.086	0.344	4794	0.93	69.75
4	20	0.108	0.434	7361	0.82	70.16
4	20	0.099	0.396	6668	1.21	70.69
5	20	0.112	0.558	14648	0.55	70.46
5	20	0.115	0.577	16929	1.17	68.90
5	20	0.088	0.442	11048	1.42	70.00

TABLE III: Errors in the mean  $H_0$  averaged over 25 realizations, for one synthetic interferometer.

$A$	$\delta_{H_0}$ [km s <sup>-1</sup> Mpc <sup>-1</sup> ]
1	0.22
2	0.16
3	0.24
4	0.51
5	0.68

- [13] A. Vecchio, Phys. Rev. D **70**, 042001 (2004).  
[14] S. A. Hughes, Mon. Not. R. Astron. Soc. **331**, 805 (2002).  
[15] C. Cutler, Phys. Rev. D **57**, 7089 (1998).  
[16] A. Sesana, F. Haardt, P. Madau, and M. Volonteri, Astrophys. J. **611**, 623 (2004).  
[17] M. Volonteri, AIP Conf. Proc. **873**, 61 (2006).  
[18] J. A. de Freitas Pacheco, C. Filloux, and T. Regimbau, Phys. Rev. D **74**, 023001 (2006).  
[19] J. R. Gair, L. Barack, T. Creighton, C. Cutler, S. L. Larson, E. S. Phinney, and M. Vallisneri, Class. and Quantum Grav. **21**, 1595 (2004).  
[20] L. Barack and C. Cutler, Phys. Rev. D **69**, 082005 (2004).  
[21] C. Hopman, AIP Conf. Proc. **873**, 241 (2006).  
[22] C. Hopman and T. Alexander, Astrophys. J. Lett. **645**, L133 (2006).  
[23] M. Dotti, R. Salvaterra, A. Sesana, M. Colpi, and F. Haardt, Mon. Not. R. Astron. Soc. **372**, 869 (2006).  
[24] M. Milosavljević and E. S. Phinney, Astrophys. J. Lett. **622**, L93 (2005).  
[25] E. S. Phinney (in preparation).  
[26] P. J. Armitage and P. Natarajan, Astrophys. J. Lett. **567**, L9 (2002).  
[27] B. Kocsis, Z. Frei, Z. Haiman, and K. Menou, Astrophys. J. **637**, 27 (2006).  
[28] B. Kocsis, Z. Haiman, K. Menou, and Z. Frei, Phys. Rev. D **76**, 022003 (2007).  
[29] B. Kocsis, Z. Haiman, and K. Menou, Astrophys. J. (submitted); Report No. arXiv:0712.1144, 2007.  
[30] J. Adelman-McCarthy *et al.*, Astrophys. J. Suppl. Ser. (submitted).  
[31] C. Stoughton *et al.*, Astron. J. **123**, 485 (2002).  
[32] M. A. Strauss *et al.*, Astron. J. **124**, 1810 (2002).  
[33] J. E. Gunn *et al.*, Astron. J. **131**, 2332 (2006).  
[34] J. E. Gunn *et al.*, Astron. J. **116**, 3040 (1998).  
[35] D. G. York *et al.*, Astron. J. **120**, 1579 (2000).  
[36] M. Fukugita, T. Ichikawa, J. E. Gunn, M. Doi, K. Shimasaku, and D. P. Schneider, Astron. J. **111**, 1748 (1996).

